

Supporting Information

Oxygen-deficient Anatase TiO₂@C Nanospindles with Pseudocapacitive Contribution for Enhancing Lithium Storage

Xiaolan Deng,^a‡ Zengxi Wei,^a‡ Chunyu Cui,^a Quanhui Liu,^a Caiyun Wang^b and Jianmin Ma^{a,c,*}

^a*School of Physics and Electronics, Hunan University, Changsha, 410082, P. R. China*

^b*ARC Centre of Excellence for Electromaterials Science, Intelligent Polymer Research Institute,
University of Wollongong, New South Wales 2522, Australia*

^c*Key Laboratory of Advanced Energy Materials Chemistry (Ministry of Education), Nankai
University, Tianjin 300071, P.R. China*

‡ X. Deng and Z. Wei contributed equally to this work.

*Corresponding author: Prof. Jianmin Ma

Email: nanoelechem@hnu.edu.cn

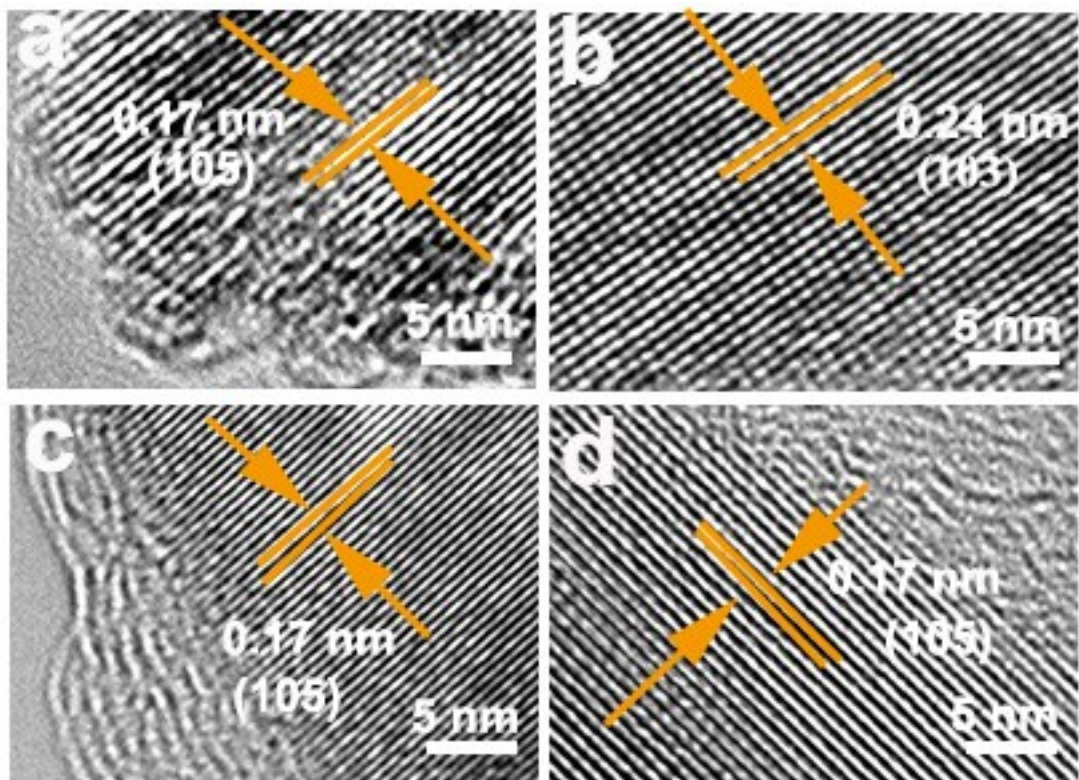


Fig. S1 (a-d) HR-TEM images of TiO_2 , H-TiO_2 , $\text{TiO}_2@\text{C}$ and $\text{H-TiO}_2@\text{C}$ nanospindles.

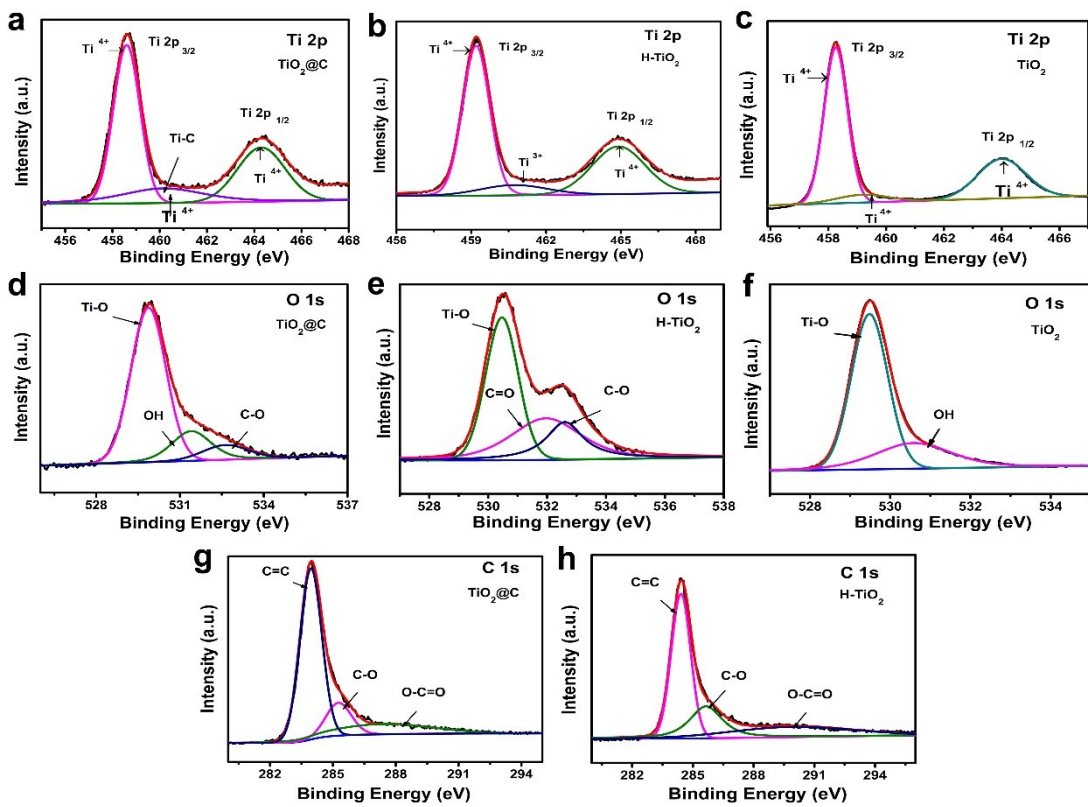


Fig. S2 (a-c) XPS spectra of Ti 2p of the $\text{TiO}_2@\text{C}$, $\text{H}-\text{TiO}_2$ and TiO_2 samples; (d-f) O 1s spectra; (g and h) C 1s spectra.

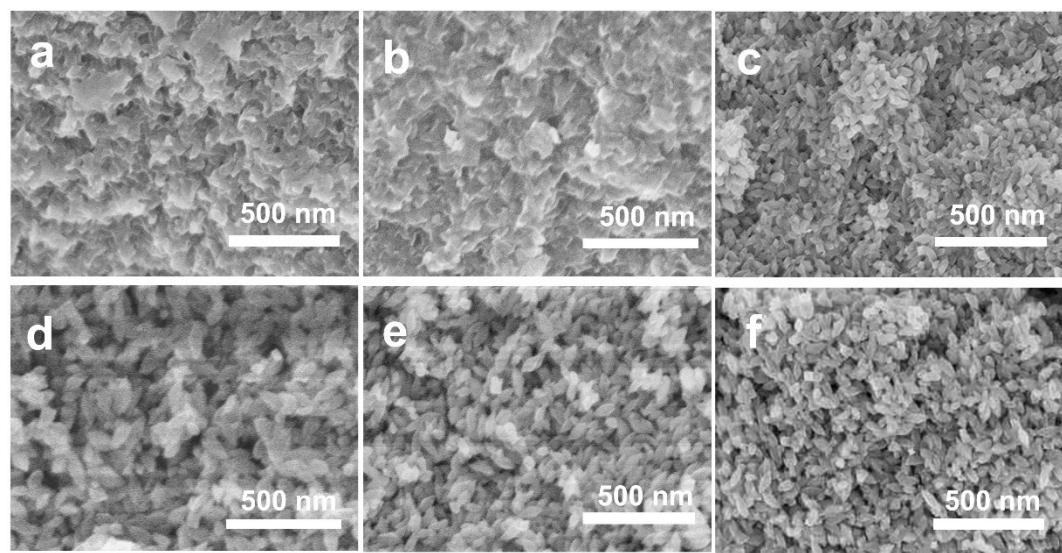


Fig. S3 SEM images of the samples obtained after different reaction times: (a) 1 h, (b) 3 h, (c) 6 h, (d) 8 h, (e) 10 h and (f) 12 h.

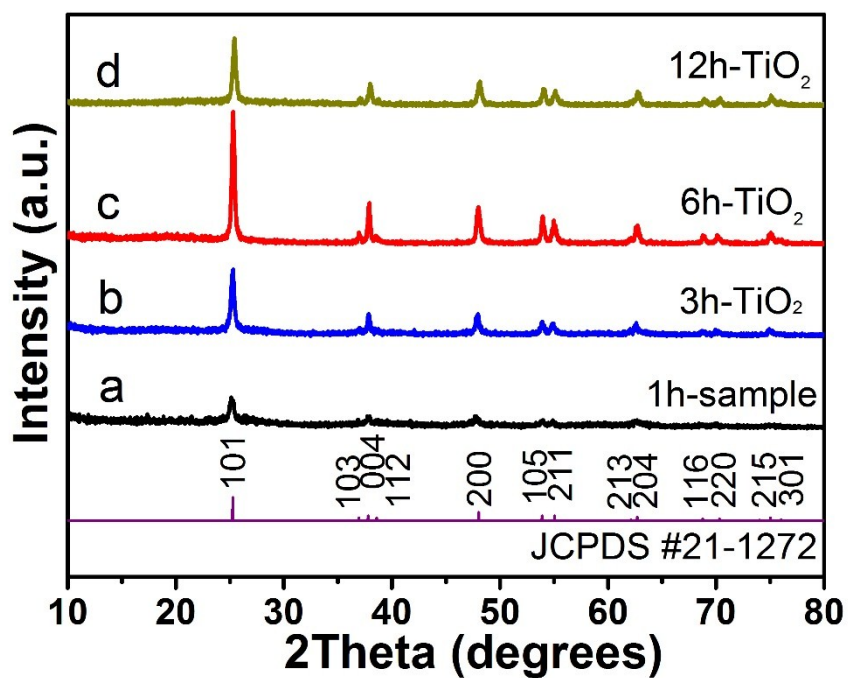


Fig. S4 The XRD patterns of the samples obtained at different reaction stages: (a)1 h; (b)3 h; (c)6 h and (c)12 h, respectively.

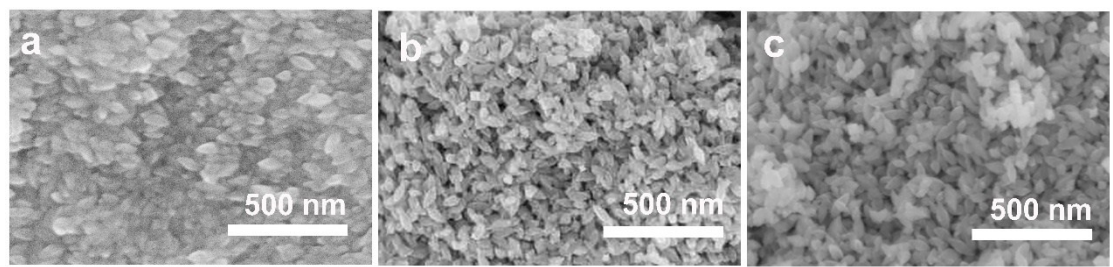


Fig. S5 SEM images of as-synthesized TiO_2 nanocrystals at (a) 100 °C, (b) 120 °C and (c) 140 °C for 12 h.

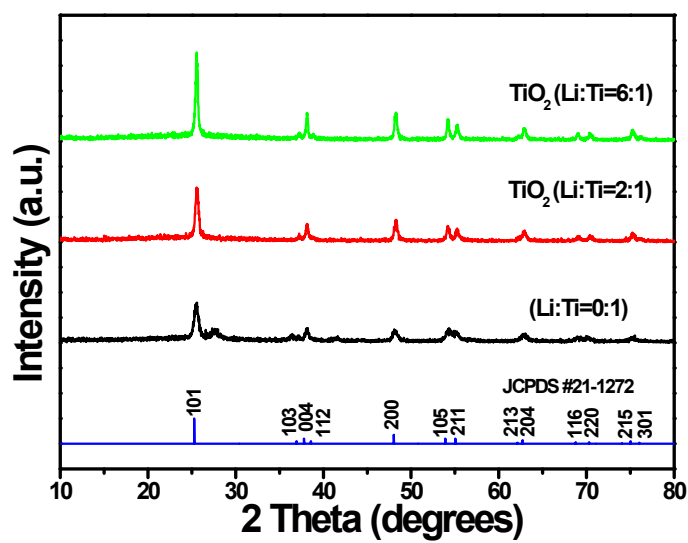


Fig. S6 XRD patterns of the products in different ratios of Li:Ti, they are 0:1, 2:1 and 6:1, respectively.

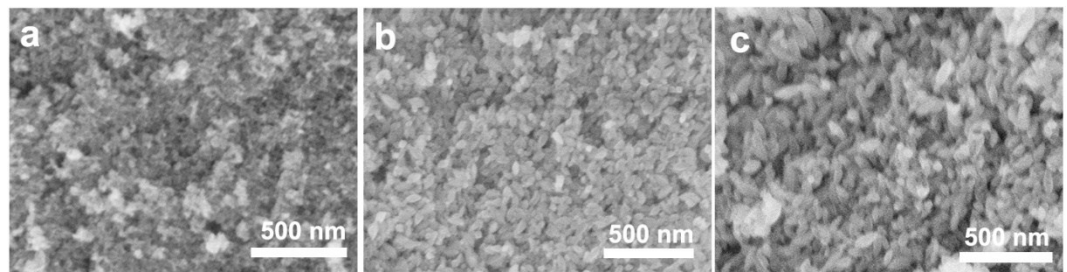


Fig. S7 SEM images the products in different ratios of Li:Ti, they are 0:1, 2:1 and 6:1, respectively.

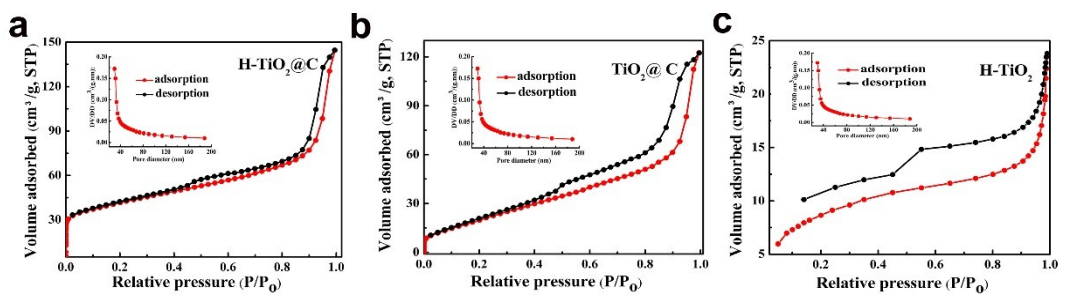


Fig. S8 N₂ adsorption–desorption isotherm and pore size distribution of (a) H-TiO₂@C, (b) TiO₂@C and H-TiO₂.

Table. S1 BET surface area and the porosity of H-TiO₂@C, TiO₂@C and H-TiO₂ samples.

Samples	BET surface area (m ² g ⁻¹)	BJH pore volume (cm ³ g ⁻¹)	Pore size (nm)
H-TiO ₂ @C	136.93	0.17	32.67
TiO ₂ @C	86.15	0.17	44.01
H-TiO ₂	51.90	0.19	75.98

In Table S1, the BET surface area and pore size of H-TiO₂@C are 136.93 m² g⁻¹ and 33.67 nm, respectively, which are higher than the TiO₂@C sample (86.15 m² g⁻¹ and 44.01 nm) and H-TiO₂ sample (51.89 m² g⁻¹ and 75.98 nm).

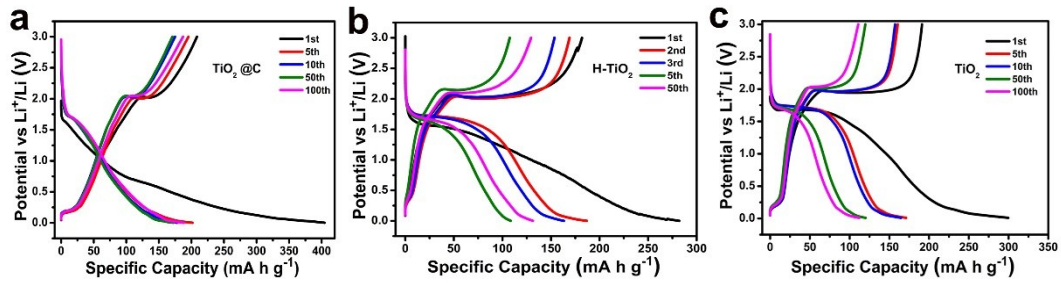


Fig. S9 Charge/discharge curves of (a) $\text{TiO}_2@\text{C}$, (b) H- TiO_2 and (c) TiO_2 electrodes at 0.1 A g^{-1} .

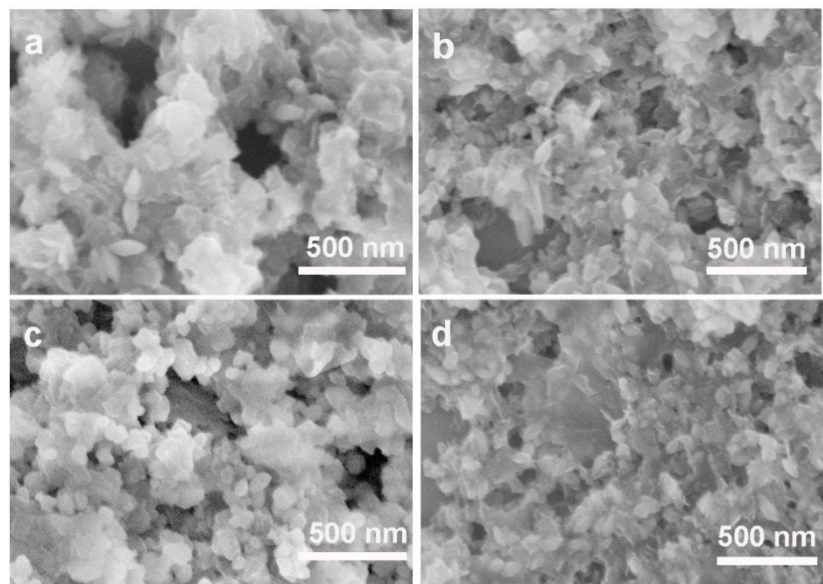


Fig. S10 SEM image of (a) H-TiO₂@C, (b) TiO₂@C, (c) H-TiO₂ and (d) TiO₂ electrodes after 150 cycles at 0.1 A g⁻¹.

Table. S2 Electrochemical performance of TiO_2 -based anode for LIBs

Ref	Samples	Current density (A g ⁻¹)	Discharge capacity (mA h g ⁻¹)	Current density (A g ⁻¹ , 1C=335 mA h g ⁻¹)					
				Rate capacity (mA h g ⁻¹)					
16	$TiO_2@C$	0.168	185.7(1 st); 145.8(200 th)	0.168	0.336	0.84	1.68	0.84	
				141	116	88	55	75	
27	rGO/TiO_2	0.1 0.5	320(1 st); 262 (100 th) 205 (500 th)	0.1	0.2	0.5	1	2	5 0.1
				262	243	212	183	151	102 262
32	$H-TiO_2$	0.2	225.6 (200 th)	0.2	0.8		1.6		3.35
				200	162		144		130
52	$TiO_2@C$	0.1	485(1 st); 286.5 (200 th)	0.1	0.2	0.5	1	0.1	
				240	205	148	95	275	
54	3D C@ TiO_2	0.067	351(1 st); 228 (120 th)	0.067	0.335	0.67	0.168	3.35	6.7 16.8
				309	226	202	169	139	100 47
55	$TiO_2@GO$	0.084 3.36	332(1 st); 205(100 th) 108(1500 th)	0.084	0.168	0.336	0.84	1.68	3.36 8.4 0.084
				~230	~210	~190	~170	~150	~130 ~100 ~220
66	$TiO_2/TiO_2(B)$	0.336	264.9(1 st); 260.1(500 th)	0.067	0.168	0.336	0.67	1.68	13.44 0.067
				~312	~287	~275	~270	~250	~181 ~315
Our work	$H-TiO_2@C$	0.1 1	797(1 st); 500(2 nd); 310 (150 th) 342(1 st); 126 (200 th)	0.1	0.168	0.34	0.68	1.68	0.1
				430	280	191	108	51	309

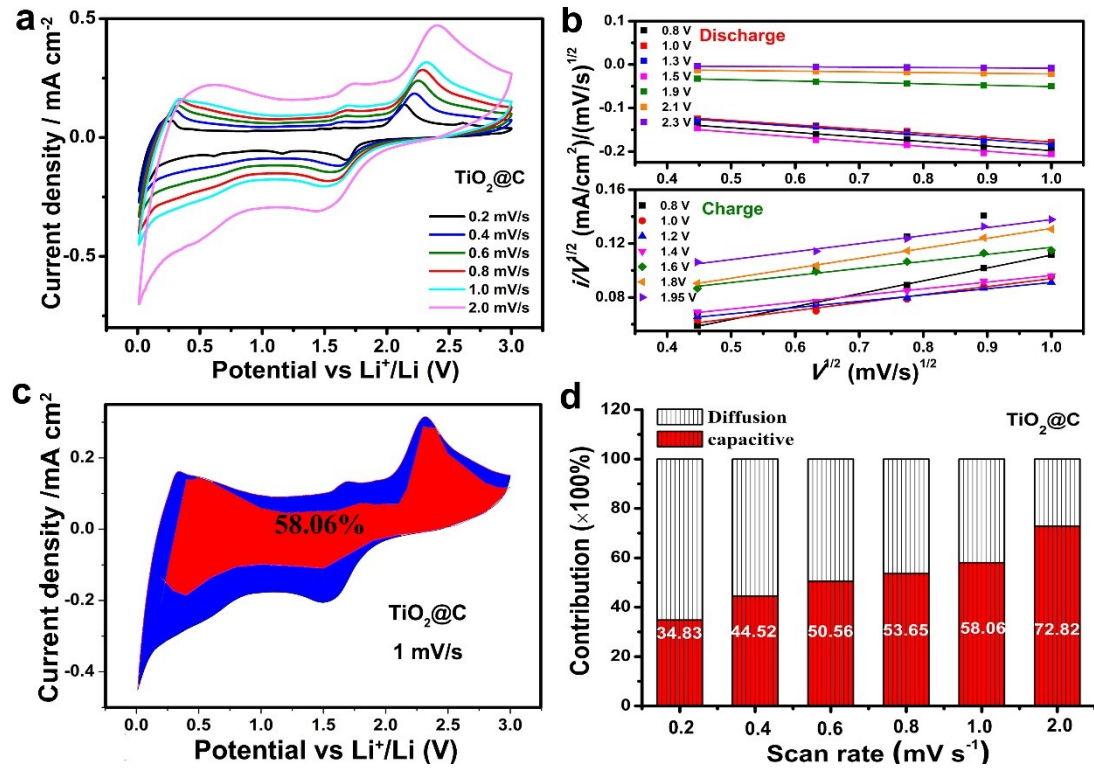


Fig. S11 Kinetic analysis of $\text{TiO}_2@\text{C}$. a) CV curves at different sweep rates. b) $i (V)/v^{1/2}$ versus $v^{1/2}$ at various potentials during charge/discharge process from 0.2 mV s^{-1} to 1 mV s^{-1} . c) Capacitive current contributions (red regions) to the charge storage at 1 mV s^{-1} . d) The contribution ratio of pseudocapacitive and diffusion-controlled current at different scan rates of $\text{TiO}_2@\text{C}$.

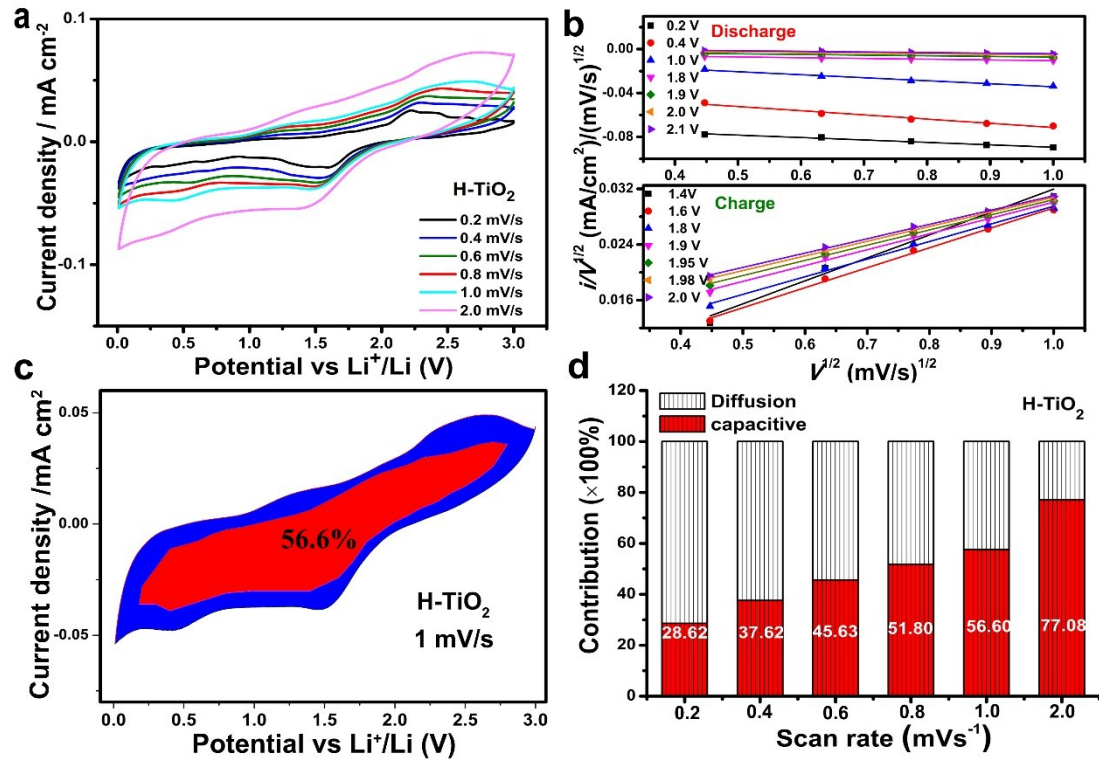


Fig. S12 Kinetic analysis of H-TiO₂ a) CV curves at different sweep rates. b) $i(V)/V^{1/2}$ versus $V^{1/2}$ at various potentials during charge/discharge process from 0.2 mV s^{-1} to 1 mV s^{-1} . c) Capacitive current contributions (red regions) to the charge storage at 1 mV s^{-1} . d) The contribution ratio of pseudocapacitive and diffusion-controlled current at different scan rates of H-TiO₂.

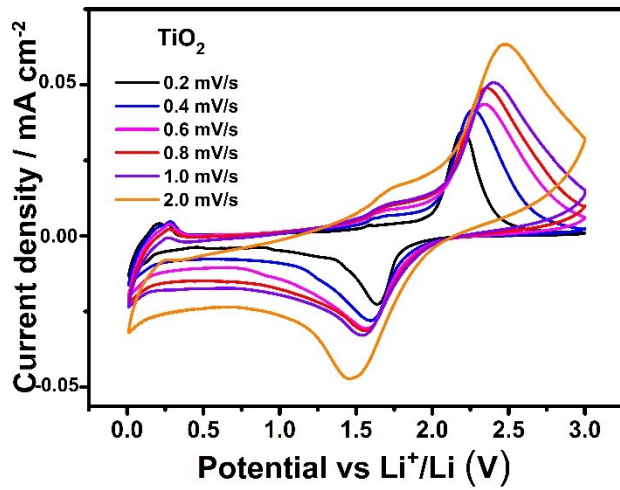


Fig. S13 Kinetic analysis of TiO_2 , CV curves at different sweep rates.